Journal of Wood Science

ORIGINAL ARTICLE

Open Access

# Radial variations of broad-sense heritability in wood properties and classification of load–deflection curves in static bending for six half-sib families of *Chamaecyparis obtusa*

Yusuke Takahashi[1,2,3], Futoshi Ishiguri[1*], Ikumi Nezu[1,2], Ryota Endo[4,5], Saki Kobayashi[5], Jun Tanabe[4], Michinari Matsushita[3], Jyunichi Ohshima[1] and Shinso Yokota[1]

## Abstract

Wood properties (annual ring width, tracheid length, microfibril angle [MFA], basic density, and air-dry density) and mechanical properties (modulus of elasticity [MOE], modulus of rupture [MOR], bending work, and compressive strength) in 34-year-old *Chamaecyparis obtusa* trees of six half-sib families were measured from pith to bark to clarify radial variations in inheritance of these traits and the relationships between wood properties and mechanical properties. In addition, within-tree and among-family differences in the load–deflection curves were discussed. Radial variations of all wood properties were fitted to linear or nonlinear mixed-effects models with random effects of families. The MFA was correlated with MOE in all radial positions, whereas air-dry density correlated with all mechanical properties in mature wood. Radial variations in broad-sense heritability differed between wood properties. A relatively higher broad-sense heritability was recognized in almost all wood properties for mature wood. Based on the results, it was concluded that mechanical properties in mature wood can be effectively improved using MFA and air-dry density as criteria. In addition, the types of load–deflection curve in mature wood differed from those in juvenile wood, suggesting that not only elastic properties, but also plastic properties in *C. obtusa* are affected by genetic controls, especially in mature wood.

**Keywords:** Hinoki cypress, Juvenile wood, Mature wood, Load–deflection curve, Tree breeding, Mechanical property

## Introduction

*Chamaecyparis obtusa* (Sieb. et Zucc.) Endl. (*hinoki* in Japanese and hinoki cypress in English) is a common coniferous plantation species in Japan. The total plantation area of this species accounts for 25% of all plantation areas (about 10 million ha) in Japan [1]. This species has been subjected to tree breeding programs managed by the Forestry Agency in Japan since the 1950s [1]. Initially, the target traits for improvement by the tree breeding programs were growth characteristics and the straightness of stems to increase wood volume, resulting in that 1070 plus trees in *C. obtusa* were selected throughout Japan by 2020. Because the wood of *C. obtusa* has been used for structural lumber, inheritance or family variations of wood properties have been investigated by several researchers [2–4]. For example, Kijidani et al. [2] reported that significant differences in microfibril angle (MFA) and basic density were found among 15 half-sib families of 29-year-old *C. obtusa* trees. Fukatsu et al. [3] also reported that the narrow-sense heritability of basic density at five annual rings from bark and six annual rings from bark to pith were 0.262 and 0.198, respectively.

*Correspondence: ishiguri@cc.utsunomiya-u.ac.jp
[1] School of Agriculture, Utsunomiya University, Utsunomiya 321-8505, Japan
Full list of author information is available at the end of the article

However, information about the inheritance of mechanical properties for *C. obtusa* is still limited.

Understanding radial variations in inheritances of wood properties is important for assessing the possibility for improvement and determining the optimal selection ages in tree breeding for wood quality [5, 6]. Radial variations of inheritance in wood properties differ among wood properties in several softwood species [3, 5–8]. Chen et al. [6] reported that the narrow-sense heritability of modulus of elasticity (MOE) for 21-year-old *Picea abies* was low near the pith and then increased continuously with final stabilization from the 10th annual ring to the bark. In half-sib families of 20-year-old *P. glauca*, narrow-sense heritability of the MFA was almost constant, between 0.25 and 0.30, over the range of cambial ages [5]. In hybrid larch (*Larix gmelinii* var. *japonica* × *L. kaempferi*), air-dry density, MOE, modulus of rupture (MOR), and compressive strength showed higher narrow-sense heritability in the bark side compared with the pith side [7]. Unfortunately, radial variations in the heritability of mechanical properties of *C. obtusa* have not yet been clarified.

When wood is subjected to bending, the relationships between loading and the corresponding deformation are expressed as a load–deflection curve. The load–deflection curve can be divided into two regions: an elastic region which is represented by a straight line, and a plastic region which is represented by a curve. The upper limit of the straight line is called the proportional limit. A higher proportional limit indicates a higher resistance to deformation by a load in the elastic region. On the other hand, the higher the maximum load, the greater the deflection in the plastic region, showing resistance to failure. Sasaki et al. [9] reported that the types of load–deflection curve in static bending varied among 36 cultivars of *Cryptomeria japonica* and could be classified into three types. We previously investigated load–deflection curves in juvenile wood of 18 full-sib families in *C. japonica* [10]. We found that the shapes of load–deflection curves were affected by genetic control, and could be classified into four types: type I showed higher load at the proportional limit and larger deflection in the plastic region, type II had intermediate load at the proportional limit and larger deflection in the plastic region, type III exhibited lower load at the proportional limit and smaller deflection in the plastic region, and type IV exhibited higher load at the proportional limit with smaller deflection in the plastic region [10]. Types of load–deflection curve should be clarified for several families in *C. obtusa* to understand not only the possibility for improvement of bending properties by tree breeding programs, but also to clarify the characteristics of this species for use as construction materials.

The objectives of the present study were to clarify radial variations of inheritance in wood properties and mechanical properties, as well as the relationships between wood properties and mechanical properties, and to identify family variations in types of load–deflection curve in static bending for *C. obtusa*. We examined wood properties and mechanical properties in six half-sib families planted in a progeny test stand located in Chiba, Japan.

## Materials and methods

### Materials

The materials in the present study were sampled from a progeny test stand located in Otaki, Chiba, Japan (35°11′16″ N, 140°13′37″ E). The progeny test stand consisted of 24 open-pollinated families which originated from first-generation plus trees selected from Kanto-Heiya districts in Kanto breeding region. The test stand was designed to include unbalanced randomized complete blocks of three replications (3600 trees/ha), and families were established in ten-tree row plots. These three blocks were established at the top, middle, and bottom of the same slope in a stand. Of the 24 families, six families (H2, K4, M5, S, S2, and T2 in Family ID) showing high survival rates and relatively superior diameter growth were selected based on the stem diameter at 1.3 m above the ground measured at 30 years of age. One individual tree with an average stem diameter and straight stem was selected from each block for each family. A total of 18 trees were felled, and logs 50 cm in length, from 0.8 m to 1.3 m above the ground, were collected at tree age of 34 years old. In this progeny test stand, the following silvicultural treatment was applied: pruning = three times up to 20 years after planting, and thinning = two times at 25 and 28 years after planting.

### Growth characteristics and stress-wave velocity in standing trees

About a month before harvesting, stem diameter at 1.3 m above the ground, tree height, and stress-wave velocity of stem were measured for about nine individuals in each family and each block; a total of 159 individuals were measured. Stress-wave propagation time was determined using a commercial handheld stress-wave timer (Fakopp Microsecond Timer, Fakopp Enterprise) according to the method of Ishiguri et al. [11]; specifically, start and stop sensors were installed, parallel to the axial direction of the stem, at upper (1.5 m above the ground) and lower (0.5 m above the ground) positions, respectively. Six measurements of stress-wave propagation time were made at the same position for each standing tree. The stress-wave velocity was calculated by dividing the distance between the two sensors by the average value of the stress-wave propagation time.

### Wood properties

Annual ring width and basic density were measured using a disk 2 cm in thickness obtained from 0.8 m above the ground for each tree. To measure the annual ring width, bark-to-bark strips (2 cm in thickness and 5 cm in width) were collected from each disk. The image data (1200 dpi) of transverse sections of the strips from pith to bark in one direction were captured by a personal computer with a scanner (GT-9300UF, EPSON, Nagano, Japan). Annual ring width was measured using image analysis software (ImageJ, National Institute of Health, Bethesda, Maryland, US). To determine the basic density, wedge-shaped specimens were also obtained from the disk without eccentricity. Small blocks were cut at 3-annual-ring intervals from pith to bark. Basic density was determined by dividing oven-dry weight at 105 ℃ by green volume determined by the water displacement method.

Bark-to-bark radial boards (3 cm in thickness) were obtained from logs 50 cm in length. To measure tracheid length and MFA, specimens (1 cm in thickness) were collected from the boards. Small blocks of latewood were prepared from one side of each specimen at the 1st annual ring and every three annual rings. These small blocks were macerated with Schultze's solution (100 mL of 35% nitric acid containing 6 g of potassium chlorate). A total of 30 tracheids in each radial position were measured using a profile projector (V-12B, Nikon, Tokyo, Japan) with a digital caliper. MFA was determined using the iodine method [12, 13] at every three annual rings from 3rd annual ring from the pith. Small-sized blocks were prepared at every three annual rings in one radial direction from pith to bark. Radial sections 20 μm in thickness were obtained from each block using a sliding microtome (REM-710, Yamato Koki, Saitama, Japan). These obtained sections were treated with Schultze's solution for 15 min, rinsed with distilled water, and dehydrated by graded ethanol series. After that, the dehydrated sections were treated with a drop of 2% iodine–potassium iodide aqueous solution, followed by a drop of 60% nitric acid. The sections were mounted with cover slips. Photomicrographs were taken by a digital camera (E-330, Olympus, Tokyo, Japan) equipped to a light microscope (CX-41, Olympus, Tokyo, Japan). At each radial position, the MFA was measured for 30 latewood tracheids on digital photomicrographs using ImageJ.

### Mechanical properties

After air-drying under conditions of 65% relative humidity and 20 ℃ for 4 months, radial boards were planed to be 20 mm in thickness. Then, boards were cut at 20-mm intervals from two radial directions from pith to bark for static bending test specimens (ca. $20 \times 20 \times 320$ mm). When preparing the specimens, the number of annual rings from the pith located in the center of the cross section of specimens was recorded. The static bending test was conducted using a universal testing machine (MSC 5/500–2, Tokyo Testing Machine, Tokyo, Japan). The loading speed and span were 5 mm/min and 280 mm, respectively. The load and deflection data were recorded using a personal computer. Static bending properties in small-clear specimens (MOE, MOR, and bending work) were calculated using the formula described in Fig. 1 [10]. After a static bending test, the specimens for air-dry density (ca. $20 \times 20 \times 20$ mm) and compressive strength parallel to grain (ca. $20 \times 20 \times 60$ mm) were prepared from each specimen without any visual defects. Air-dry density was calculated by dividing the air-dry weight by the volume of the obtained specimens in the air-dry condition. The compressive test was conducted using a universal testing machine (RTF-2350, A&D, Tokyo, Japan) with a load speed of 0.5 mm/min. Compressive strength was calculated from the maximum load (N) by dividing it by the cross-sectional area ($mm^2$). The moisture contents of all specimens for the static bending test and compressive test were measured. The mean values and standard deviations for bending and compressive strength were $10.6 \pm 1.5\%$ and $11.6 \pm 0.7\%$, respectively.

### Data analysis

All statistical analyses were performed using the open-source statistical software R, version 4.0.3 [14]. To

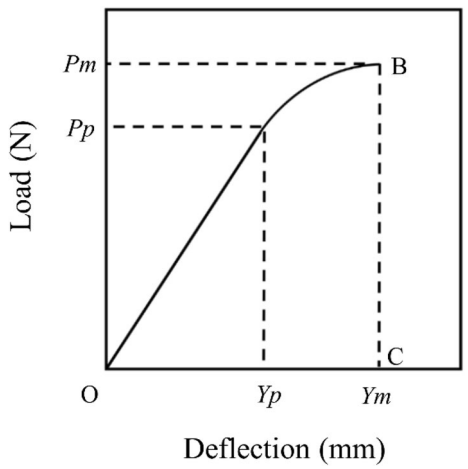


**Fig. 1** Calculation of static bending properties from load–deflection curve of static bending test [10]. *Pm*, maximum load; *Pp*, load at proportional limit; *Ym*, maximum deflection; *Yp*, deflection at proportional limit. MOE and MOR were determined by the following equations: MOE (GPa) = $Ppl^3/4Ypbh^3$, MOR (MPa) = $3Pml/2bh^2$, where *l* is the span, *b* is the width of the specimen, *h* is the height of the specimen, bending work is an area enclosed with OBC in this graph.

evaluate the effects of genetics, environment, and their interaction on growth characteristics and stress-wave velocity, the following linear mixed-effects model was developed using the lmer function in the lme4 package [15]:

$$y_{ij} = \mu + G_i + B_j + G_iB_j + e_{ij}, \quad (1)$$

where $y_{ij}$ is the measured values of tree height, stem diameter, or stress-wave velocity in the $i$th family of the $j$th block, $\mu$ is the mean value, $G_i$ and $B_j$ are the random effects of the $i$th family and the $j$th block, $G_iB_j$ is the random effect of interaction between the $i$th family and the $j$th block, and $e_{ij}$ is the residual.

The genetic effect on the overall mean and mean of each radial position was estimated using the following linear mixed-effects model formula:

$$y_i = \mu + G_i + e_i, \quad (2)$$

where $y_i$ is the measured values of wood properties in overall or radial positions in the $i$th family, $\mu$ is the mean value, $G_i$ is the random effect of the $i$th family, and $e_i$ is the residual. Because the number of individuals per family for each block was limited, the effect of the block was not considered in this model.

Linear and nonlinear mixed-effects models were used to evaluate the radial variations of wood properties in relation to the annual ring number from the pith using the lmer function in the lme4 package and the nlme function in the nlme package [16]. The following two full models were developed and compared:

Model I (linear model):

$$y_{ij} = (\beta_0 + b_{0j})x_{ij} + \beta_1 + b_{1j} + e_{ij}, \quad (3)$$

Model II (nonlinear model):

$$y_{ij} = \frac{(\beta_0 + b_{0j})x_{ij}}{(\beta_1 + b_{1j}) + x_{ij}} + \beta_2 + b_{2j} + e_{ij}, \quad (4)$$

where $y_{ij}$ is the measured value for the $i$th annual ring of the $j$th family; $x_{ij}$ is the $i$th annual ring number from the pith of the $j$th family; $\beta_0$, $\beta_1$, and $\beta_2$ are the fixed-effects parameters; $b_{0j}$, $b_{1j}$, and $b_{2j}$ are random-effects parameters of the $j$th family; and $e_{ij}$ is the residual. Model II was based on the Michaelis–Menten equation [17, 18]. In Model II, $\beta_0$, and $\beta_2$ represent the rate and the intercept parameters, respectively. The higher or lower asymptotes are given by $\beta_0 + \beta_2$ [17]. The full models of Model I and Model II did not converge for all wood properties, while the models with one random effect converged for all wood properties. Thus, a total of two linear mixed-effects models and three nonlinear mixed-effects models were used to evaluate the radial variations of wood properties. For comparison, models without random effects were also used. Based on the model selection approach, the Akaike information criterion (AIC) [19] was used to select the more parsimonious model for each wood property trait among the linear or nonlinear models with or without the family-specific random-effects parameters. If a model including one or more family-specific random-effects parameters was selected, we considered that there was a considerable among-family variation in the radial variation of a wood property trait. The AIC was calculated using the following formula:

$$\mathrm{AIC} = -2\ln(L) + 2m, \quad (5)$$

where $\ln(L)$ is the log-likelihood of the model and $m$ is the number of estimated parameters.

The boundary between juvenile wood and mature wood for each individual tree was determined using tracheid length in each annual ring estimated by a regression formula based on the optimal nonlinear mixed-effects model.

The broad-sense heritability ($H^2$) was calculated using the following formula:

$$H^2 = \frac{\sigma_f^2}{\sigma_f^2 + \sigma_e^2}, \quad (6)$$

where $\sigma_f^2$ and $\sigma_e^2$ are variance components of family and residuals, respectively. These variance components were estimated using the linear mixed-effects models of Eqs. (1) and (2).

To evaluate the radial variations of $H^2$ and relationships between radial positions, mean values of all wood properties in each individual tree were calculated for four radial positions (from 1st to 6th, 7th to 12th, 13th to 21st, and 22nd to 34th annual rings from the pith). The relationships between wood properties were determined using Pearson's correlation coefficient.

Principal component analysis and cluster analysis were employed to categorize the families with respect to differences in load–deflection curves. The methods were the same as those of our previous study [10]. Principal component scores were calculated using a correlation matrix with the four following variables: arithmetic family mean values in load at the proportional limit, deflection at the proportional limit, maximum load and maximum deflection. Using the first and second principal component scores from principal component analysis as variables, cluster analysis using the Ward hierarchical clustering algorithm was performed to categorize six families. The optimal number of clusters was determined by the Jain–Dubes method [20].

## Results and discussion

### Growth characteristics and stress-wave velocity of stems

Table 1 shows broad-sense heritability and variance components in growth characteristics and stress–wave velocity of stems. In tree height, relatively higher variance components were found in block (0.36) and interaction (0.37) terms, whereas that of family was quite low (0.00). In contrast, the highest variance component in stress-wave velocity was found in family (0.17). The ratios of family, block, and interaction terms in stem diameter were 0.04, 0.00, and 0.09, respectively. The broad-sense heritability of stress-wave velocity ($H^2 = 0.18$) was higher than those of growth characteristics. These results indicated that growth characteristics are sensitive to environmental differences among sites of slope in a stand, whereas mechanical properties are mainly affected by the genetic factors rather than those environmental factors. A similar tendency for *C. obtusa* was reported by Fukatsu et al. [3]. Thus, mechanical properties could be more effectively improved by tree breeding than by growth characteristics in *C. obtusa*.

### Wood properties

The overall mean values of wood properties in the sampled trees are shown in Table 2. The mean values obtained in the present study were similar to those of previous studies in *C. obtusa* (Table 3) [4, 21–25].

Radial variations in wood properties were fitted to linear and nonlinear mixed-effects models (Model I and Model II, respectively). Table 4 shows a comparison of AIC values obtained from linear and nonlinear mixed-effects models. Based on the results of AIC values, MOR, bending work, and compressive strength were fitted to a linear mixed-effects model with random effects (Model I), whereas the other wood properties were adapted to a nonlinear mixed-effects model with random effects of families (Model II). The results suggest that for the values that were fitted by the linear model, MOR gradually increased, and bending work and compressive strength gradually decreased from the pith to bark. Tracheid

**Table 2** Statistical values and broad-sense heritability of measured traits

| Trait | Mean ($n = 18$) | SD ($n = 18$) | Min | Max | $H^2$ |
|---|---|---|---|---|---|
| Stem diameter (cm) | 20.0 | 2.0 | 18.5 (S) | 21.1 (M5) | – |
| Tree height (m) | 11.1 | 2.5 | 9.3 (S) | 12.6 (M5) | – |
| SWV (km/s) | 3.41 | 0.24 | 3.09 (H2) | 3.60 (S2) | – |
| ARW (mm) | 2.8 | 0.3 | 2.5 (S) | 3.0 (M5) | 0.02 |
| TL (mm) | 2.20 | 0.10 | 2.10 (S) | 2.32 (T2) | 0.39 |
| MFA (degree) | 17.8 | 3.1 | 14.8 (S2) | 22.7 (H2) | 0.48 |
| BD (g/cm$^3$) | 0.404 | 0.017 | 0.391 (T2) | 0.414 (S) | 0.00 |
| AD (g/cm$^3$) | 0.474 | 0.025 | 0.450 (T2) | 0.507 (M5) | 0.21 |
| MOE (GPa) | 7.42 | 1.04 | 5.89 (H2) | 8.24 (S2) | 0.50 |
| MOR (MPa) | 80.8 | 6.9 | 73.4 (H2) | 86.5 (S) | 0.18 |
| W (N m) | 9.15 | 1.82 | 7.53 (K4) | 11.25 (S) | 0.47 |
| CS (MPa) | 39.3 | 3.2 | 34.8 (H2) | 41.0 (M5) | 0.20 |

*SD* standard deviation, *Min*. minimum family mean, *Max*. maximum family mean, $H^2$ broad-sense heritability, *n* number of trees, *SWV* stress-wave velocity, *ARW* annual ring width, *TL* tracheid length, *MFA* microfibril angle, *BD* basic density, *AD* air-dry density, *MOE* modulus of elasticity, *MOR* modulus of rupture, *W* bending work, *CS* compressive strength

The characters in parentheses indicate Family ID showing minimum or maximum mean values

The values of $H^2$ for stem diameter, tree height, and stress-wave velocity are listed in Table 1

**Table 1** Family mean values and ratio of variance components for traits measured in standing trees

| Family ID | *n* | D (cm) | | TH (m) | | SWV (km/s) | |
|---|---|---|---|---|---|---|---|
| | | Mean | SD | Mean | SD | Mean | SD |
| H2 | 27 | 21.1 | 3.4 | 11.3 | 2.0 | 3.23 | 0.25 |
| K4 | 27 | 19.4 | 2.5 | 10.3 | 1.1 | 3.38 | 0.24 |
| M5 | 26 | 20.6 | 3.4 | 11.5 | 2.3 | 3.22 | 0.22 |
| S | 27 | 18.6 | 3.2 | 10.4 | 1.7 | 3.36 | 0.23 |
| S2 | 25 | 19.4 | 2.9 | 11.0 | 1.2 | 3.47 | 0.20 |
| T2 | 27 | 20.9 | 2.8 | 12.0 | 2.8 | 3.48 | 0.18 |
| Mean | 159 | 20.0 | 3.2 | 11.1 | 2.0 | 3.36 | 0.24 |
| $H^2$ | | 0.07 | | 0.07 | | 0.18 | |
| $V_f$ | | 0.04 | | 0.00 | | 0.17 | |
| $V_b$ | | 0.00 | | 0.36 | | 0.07 | |
| $V_{fb}$ | | 0.09 | | 0.37 | | 0.04 | |
| $V_r$ | | 0.87 | | 0.27 | | 0.72 | |

*n* number of trees, *D* stem diameter at 1.3 m above the ground, *TH* tree height, *SWV* stress-wave velocity, *SD* standard deviation, $H^2$ broad-sense heritability

$V_f$, $V_b$, $V_{fb}$, and $V_r$ represent variance components ratio of family, block, interaction between family and block, and residual, respectively

length, MFA, basic density, air-dry density, and MOE, which were explained by the nonlinear model, changed up to a few annual rings from the pith and then stabilized toward the bark (Fig. 2). Tracheid length and MFA change rapidly near the pith, and they become constant toward the bark in many softwood species [26–28], including *C. obtusa* [2, 23, 29]. This tendency in tracheid length and MFA was also observed in the present study. Kijidani et al. [2] reported that basic density in 29-year-old *C. obtusa* was larger near the pith and became smaller toward the bark side. Radial variations in basic density and air-dry density obtained in the present study also showed similar trends to those of the basic density reported by Kijidani et al. [2].

Radial variations in wood properties differed among families and clones in a species [2, 30]. Tanabe et al. [30] found that radial variation patterns of MOR in *Picea jezoensis* varied among 10 families. In addition, the rate

**Table 3** Comparison of wood properties of *C. obtusa* grown in Japan

| Place | Tree age | ARW (mm) | TL (mm) | MFA (degree) | BD (g/cm$^3$) | AD (g/cm$^3$) | MOE (GPa) | MOR (MPa) | CS (MPa) | Reference |
|---|---|---|---|---|---|---|---|---|---|---|
| Chiba | 34 | 2.8 | 2.2 | 17.8 | 0.404 | 0.474 | 7.42 | 80.8 | 39.3 | Present study |
| Chiba | 17 | 1.3–4.0 | 1.6–2.8 | 15–28 | 0.38–0.43 | | | | | [21] |
| Fukuoka | 25 | | 1.77–2.55 | | 0.422 | | | | 43.4 | [22] |
| Tochigi | 27 | 2.84 | 2.27 | 14.3 | 0.42 | | 8.5 | 88.4 | | [23] |
| Oita | 20–32 | | | | 0.356–0.465 | 0.44–0.49 | 7.47–9.56 | 73.8–90.5 | | [24] |
| Kochi | 115–120 | | | | | 0.477 | 10.7 | 82.4 | 40.6 | [25] |
| Miyazaki | 37 | | 1.7–3.6 | 8.1–32.0 | 0.325–0.458 | | 6.8–15.5 | 72–116 | | [4] |

*ARW* annual ring width, *TL* tracheid length, *MFA* microfibril angle, *BD* basic density, *AD* air-dry density, *MOE* modulus of elasticity, *MOR* modulus of rupture, *CS* compressive strength

**Table 4** Comparison of AIC values in the linear and nonlinear mixed-models for radial variations in relation to cambial age

| Model formula | | | | Random effect | | | AIC for each wood property trait | | | | | | | |
|---|---|---|---|---|---|---|---|---|---|---|---|---|---|---|
| | $\beta_0$ | $\beta_1$ | $\beta_2$ | $b_{0j}$ | $b_{1j}$ | $b_{2j}$ | TL | MFA | BD | AD | MOE | MOR | W | CS |
| Ia:$y_{ij} = \beta_1 + e_{ij}$ | | ✓ | | | | | 361 | 1105 | − 1589 | − 458 | 588 | 1178 | 812 | 843 |
| Ib:$y_{ij} = \beta_0 x_{ij} + \beta_1 + e_{ij}$ | ✓ | ✓ | | | | | 67 | 1044 | − 1925 | − 528 | 538 | 1172 | 813 | 840 |
| Ic:$y_{ij} = \beta_0 x_{ij} + \beta_1 + b_{1j} + e_{ij}$ | ✓ | ✓ | | | ✓ | | 105 | 1081 | − 1977 | − 539 | 505 | **1144** | **802** | **758** |
| Id:$y_{ij} = (\beta_0 + b_{0j}) x_{ij} + \beta_1 + e_{ij}$ | ✓ | ✓ | | ✓ | | | 367 | 1026 | − 1954 | − 582 | 508 | 1148 | 815 | 795 |
| Ie:$y_{ij} = (\beta_0 + b_{0j}) x_{ij} + \beta_1 + b_{1j} + e_{ij}$ | ✓ | ✓ | | ✓ | ✓ | | 104 | 1019 | − 1975 | − 584 | 503 | 1149 | 806 | 765 |
| IIa:$y_{ij} = \frac{\beta_0 x_{ij}}{\beta_1 + x_{ij}} + \beta_2 + e_{ij}$ | ✓ | ✓ | ✓ | | | | − 55 | 1004 | − 2097 | − 534 | 523 | 1168 | – | – |
| IIb:$y_{ij} = \frac{\beta_0 x_{ij}}{\beta_1 + x_{ij}} + \beta_2 + b_{2j} + e_{ij}$ | ✓ | ✓ | ✓ | | | ✓ | − 74 | **888** | **− 2282** | **− 617** | 425 | – | – | – |
| IIc:$y_{ij} = \frac{\beta_0 x_{ij}}{(\beta_1 + b_{1j}) + x_{ij}} + \beta_2 + e_{ij}$ | ✓ | ✓ | ✓ | | ✓ | | **− 85** | 999 | − 2255 | – | 520 | – | – | – |
| IId:$y_{ij} = \frac{(\beta_0 + b_{0k}) x_{ij}}{\beta_1 + x_{ij}} + \beta_2 + e_{ij}$ | ✓ | ✓ | ✓ | ✓ | | | − 71 | – | − 2274 | − 429 | **423** | – | – | – |

- developed model did not converge

Random-effects term $b_{0j}$ in both models corresponded to slope parameters in the regression line or curve. Random-effects terms $b_{1j}$ in Model II and $b_{2j}$ in Model II corresponded to intercept parameters in the regression line or curve

*TL* tracheid length, *MFA* microfibril angle, *BD* basic density, *AD* air-dry density, *MOE* modulus of elasticity, *MOR* modulus of rupture, *W* bending work, *CS* compressive strength

The bold style values indicate the smallest AIC values among the developed models for each of the examined wood properties

(See figure on next page.)

**Fig. 2** Radial variations of wood properties in individual trees. Number of trees = 18. TL, tracheid length; MFA, microfibril angle; BD, basic density; AD, air-dry density; MOE, modulus of elasticity; MOR, modulus of rupture; W, bending work; CS compressive strength. The solid lines or curves indicate the regression lines or curves of fixed-effect parameters in the selected models. Values in parentheses indicate the standard errors of each fixed effect.

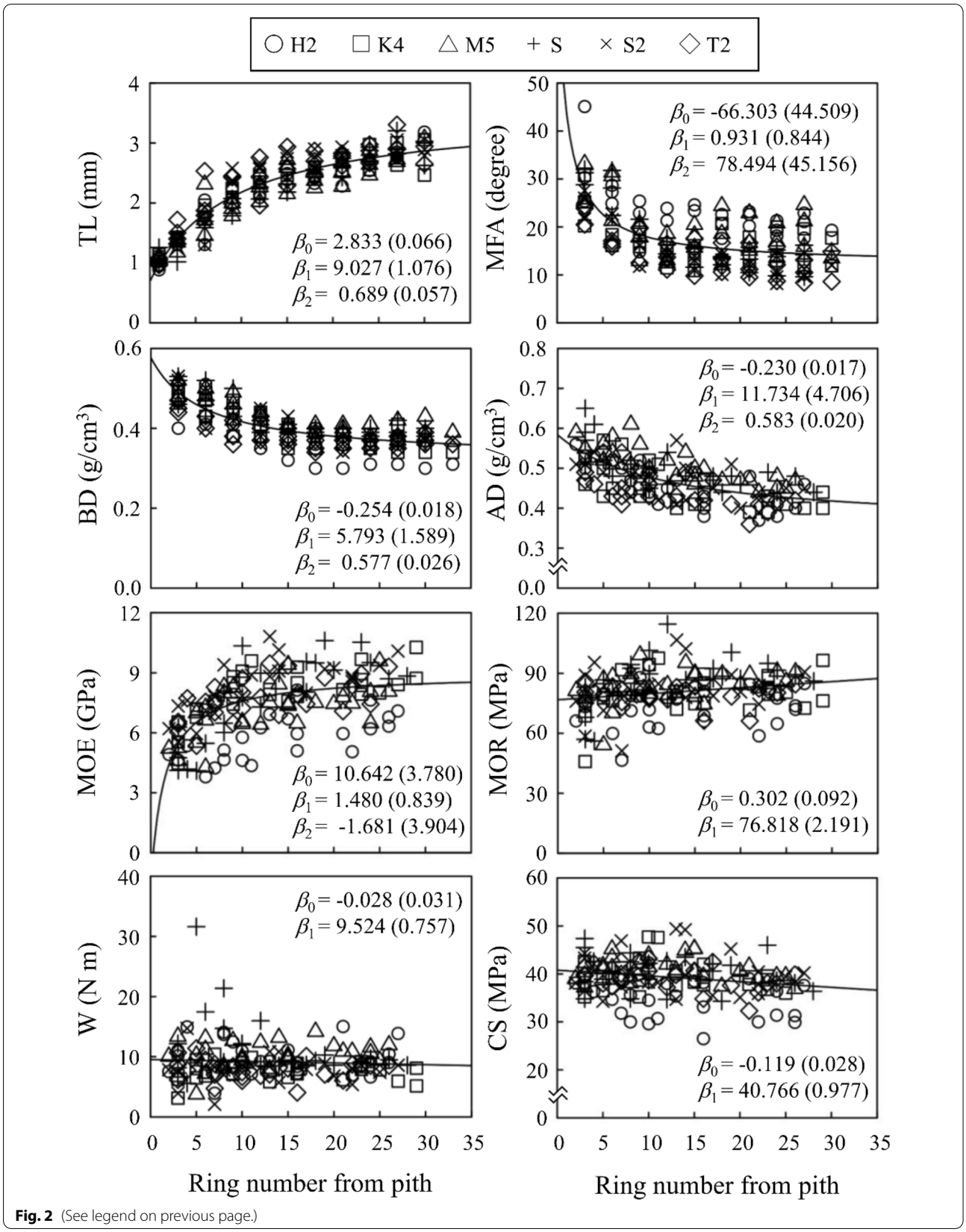


**Fig. 2** (See legend on previous page.)

of decrease from pith to bark of MFA and basic density differed among 15 half-sib families of *C. obtusa* [2]. In the present study, linear and nonlinear mixed-effects models with random effects of family were applied to radial variations of wood properties to evaluate among-family variations in radial variation. The optimal model includes the random effect of family, suggesting that radial variations of wood properties vary among-family. As shown in Table 4, the best model for MOE included random effects of families in slope ($b_{0j}$ in Model IId), suggesting that the rate at which MOE increases (rapidly, from the pith until MOE stabilizes) varies among families. Therefore, wood with more stable MOE from pith to bark could be obtained by family selection in tree breeding. On the other hand, radial variations of other wood properties except for tracheid length fitted the models with random effects of family with regard to intercept (Model Ic and Model IIb). These results indicate that the overall means of wood properties from pith to bark vary among families, whereas radial patterns might not vary among families.

In softwood species, wood properties differ dramatically between juvenile and mature wood [4, 26, 28, 31]. Tracheid length has been used as a trait to determine the boundary between juvenile wood and mature wood [31–33]. Shiokura [32] used a logarithmic formula to describe the radial variation of tracheid length, and he also pointed out that for distinguishing between juvenile and mature wood, 1% of the increasing rate for tracheid length was desirable. In the present study, the boundary between juvenile and mature wood was determined based on the radial variation of tracheid length described by a nonlinear mixed-effects model based on the Michaelis–Menten equation (Model IIc in Table 4). The results showed that the boundary between juvenile and mature wood for each tree ranged between the 19th and 25th annual rings from the pith (Table 5). The boundary age obtained in the present study was similar to that of previous studies on other species [31–33]. Although the estimated boundary varies due to species, age, or methods, a nonlinear mixed-effects model based on the Michaelis–Menten equation is an alternative tool for determining the boundary between juvenile and mature wood with various random effects, such as environmental and genetic factors.

**Table 5** Boundary between juvenile and mature wood based on radial variation of latewood tracheid length

| Family ID | Sample tree | $b_{1j}$ | Boundary annual ring number |
|---|---|---|---|
| H2 | 1 | 1.42 | 24 |
| | 2 | − 0.39 | 22 |
| | 3 | 0.79 | 24 |
| K4 | 1 | 1.22 | 24 |
| | 2 | − 0.43 | 22 |
| | 3 | − 1.22 | 22 |
| M5 | 1 | 0.84 | 24 |
| | 2 | − 0.33 | 23 |
| | 3 | 2.93 | 25 |
| S | 1 | 2.53 | 25 |
| | 2 | 0.81 | 24 |
| | 3 | 0.88 | 24 |
| S2 | 1 | − 0.94 | 22 |
| | 2 | − 1.69 | 21 |
| | 3 | − 1.89 | 21 |
| T2 | 1 | − 1.81 | 21 |
| | 2 | − 3.21 | 19 |
| | 3 | 0.49 | 23 |
| Broad-sense heritability | | | 0.51 |

$b_{1j}$, random-effects parameter of the $j$th family

Tracheid length at every annual ring was estimated by Model II with random-effects parameter $b_{1j}$

The annual ring number at the boundary was regarded as the annual ring number at which the annual increment of tracheid length became less than 1%

## Relationships between wood properties and mechanical properties

The relationships between MFA or wood density and mechanical properties have been reported in many softwood species. In addition, the contributions of wood properties to mechanical properties vary due to species and/or radial positions (e.g., juvenile and mature wood) [7, 34, 35]. In 29-year-old hybrid larch (*L. gmelinii* × *L. kaempferi*), Fujimoto et al. [7] reported that correlation coefficients between air-dry density and MOE, MOR, or compressive strength were high values. In *Pinus radiata*, MOE was highly correlated with MFA rather than wood density [34]. In comparison with the contributions of MFA or wood density to MOE, Cown et al. [35] also reported that in *P. radiata*, the effect of MFA on MOE was larger than that of wood density in juvenile wood, whereas wood density showed a greater influence in mature wood. In the present study, the correlation coefficients between MFA or air-dry density and mechanical properties were estimated at four radial positions (Table 6). At all radial positions, MOE was mainly affected by MFA, whereas compressive strength was largely influenced by air-dry density. The high correlation coefficients between air-dry density and bending properties were obtained in outer radial positions (22nd–34th radial position in MOE, and 13th–21st and 22nd–34th radial positions in MOR and bending work). These results are in agreement with those of *P. radiata* [35]. The results of the present study showed that both MFA and

**Table 6** Correlation coefficients between microfibril angle (MFA) or air-dry density (AD) and mechanical properties at each radial position

| Factor | Radial position | MOE | MOR | W | CS |
|---|---|---|---|---|---|
| MFA | 1st–6th | **– 0.699** (0.001) | – 0.376 (0.124) | 0.391 (0.109) | – 0.197 (0.447) |
| | 7–12th | **– 0.784** (< 0.001) | – 0.205 (0.416) | 0.308 (0.214) | **– 0.690** (0.001) |
| | 13th–21st | **– 0.826** (< 0.001) | **– 0.501** (0.034) | 0.198 (0.431) | – 0.396 (0.104) |
| | 22nd–34th | **– 0.803** (< 0.001) | – 0.434 (0.071) | 0.445 (0.064) | **– 0.484** (0.041) |
| AD | 1st–6th | 0.111 (0.660) | 0.341 (0.166) | 0.049 (0.847) | **0.651** (0.004) |
| | 7th–12th | 0.294 (0.236) | 0.381 (0.119) | 0.234 (0.349) | **0.649** (0.003) |
| | 13th–21st | 0.322 (0.193) | **0.737** (< 0.001) | **0.649** (0.003) | **0.787** (< 0.001) |
| | 22nd–34th | **0.503** (0.023) | **0.860** (< 0.001) | **0.630** (0.005) | **0.829** (< 0.001) |

Number of sample trees = 18

*MOE* modulus of elasticity, *MOR* modulus of rupture, *W* bending work, *CS* compressive strength

The values indicate correlation coefficients

The values in parentheses indicate *p*-values

The values in bold indicate correlation coefficients with a significance less than 0.05 levels

**Table 7** Age–age correlations between the mean of all radial positions and each radial position for all traits

| Trait | Radial Position | | | |
|---|---|---|---|---|
| | 1st–6th | 7–12th | 13th–21st | 22nd–34th |
| ARW | **0.538** (0.021) | **0.724** (< 0.000) | 0.212 (0.397) | 0.303 (0.221) |
| TL | **0.652** (0.003) | **0.839** (< 0.000) | **0.947** (< 0.000) | **0.773** (< 0.000) |
| MFA | **0.859** (< 0.000) | **0.797** (< 0.000) | **0.927** (< 0.000) | **0.922** (< 0.000) |
| BD | **0.580** (0.011) | 0.443 (0.065) | 0.412 (0.089) | **0.686** (0.001) |
| AD | **0.920** (< 0.000) | **0.904** (< 0.000) | **0.881** (< 0.000) | **0.876** (< 0.000) |
| MOE | **0.752** (< 0.000) | **0.931** (< 0.000) | **0.901** (< 0.000) | **0.918** (< 0.000) |
| MOR | **0.730** (< 0.000) | **0.745** (< 0.000) | **0.748** (< 0.000) | **0.905** (< 0.000) |
| W | **0.671** (0.002) | **0.787** (< 0.000) | **0.623** (0.005) | **0.740** (< 0.000) |
| CS | **0.843** (< 0.000) | **0.896** (< 0.000) | **0.927** (< 0.000) | **0.912** (< 0.000) |

Number of sample trees = 18

*ARW* annual ring width, *TL* tracheid length, *MFA* microfibril angle, *BD* basic density, *AD* air-dry density, *MOE* modulus of elasticity, *MOR* modulus of rupture, *W* bending work, *CS* compressive strength

The values indicate correlation coefficients

The values in parentheses indicate *p*-values

The values in bold indicate correlation coefficients with a significance level less than 0.05

air-dry density were crucial factors required to improve mechanical properties in *C. obtusa*. Although the contributions of the effects of wood properties on mechanical properties vary due to mechanical properties and radial positions, if the target traits are all mechanical properties in mature wood, they might be effectively improved using both MFA and air-dry density as indicators for the selection of trees.

Table 7 shows the correlation coefficients between the overall mean values and mean values at each radial position for all wood properties. Higher-valued and significant age–age correlations were obtained for almost all wood properties at all radial positions. Tanabe et al. [30] reported that the overall mean values of annual ring width, air-dry density, MOE, and MOR in *P. jezoensis* can be estimated by the mean values of those in radial positions from the 11th to 15th annual rings from the pith. The results obtained in the present study suggest that early selection for all wood properties is possible in *C. obtusa*, even at very early ages, such as less than six years old.

### Broad-sense heritability of wood properties

Values of broad-sense heritability estimated from the overall radial positions of wood properties are listed in Table 2. Moderate-to-high broad-sense heritability ($H^2 = 0.18–0.50$) was found for all wood properties, except for annual ring width ($H^2 = 0.02$) and basic density ($H^2 = 0.00$). These results are also supported by previous reports in which wood properties were found to be heritable traits [3, 5–7, 10, 36].

Heritability varies from pith to bark in some softwood species [3, 5–7]. In tracheid length, the highest heritability was shown in the 13th–21st radial position (Table 8). In addition, the heritability of the boundary between juvenile and mature wood determined by radial variation of tracheid length was also high value ($H^2 = 0.51$, Table 5). This result suggests that increasing mature wood volume in this species could be possible through family selection. On the other hand, the broad-sense heritability of annual ring width and basic density were almost zero or low at all radial positions (Table 8). In MFA and MOE, all radial positions except for the 7–12th radial position showed high heritability (Table 8). On the other hand, the heritability of MOR increased from the pith side to

**Table 8** Broad-sense heritability of all traits at each radial position

| Trait | Radial position | | | |
|---|---|---|---|---|
| | 1st–6th | 7–12th | 13th–21st | 22nd–34th |
| ARW | 0.00 | 0.00 | 0.00 | 0.00 |
| TL | 0.09 | 0.48 | 0.54 | 0.21 |
| MFA | 0.54 | 0.01 | 0.51 | 0.61 |
| BD | 0.00 | 0.00 | 0.26 | 0.00 |
| AD | 0.10 | 0.02 | 0.01 | 0.52 |
| MOE | 0.47 | 0.18 | 0.60 | 0.66 |
| MOR | 0.01 | 0.10 | 0.23 | 0.40 |
| W | 0.00 | 0.63 | 0.36 | 0.36 |
| CS | 0.13 | 0.00 | 0.07 | 0.40 |

*ARW* annual ring width, *TL* tracheid length, *MFA* microfibril angle, *BD* basic density, *AD* air-dry density, *MOE* modulus of elasticity, *MOR* modulus of rupture, *W* bending work, *CS* compressive strength

the bark side, and the heritability of bending work was relatively higher in 7–34th radial positions (Table 8). The low heritability of annual ring width may be due to the sampling strategy in this study, in which families with a relatively larger stem diameter were used, resulting in no differences in radial growth rate among the six families. The results of radial variations in heritability indicate that genetic influence on wood properties might differ among radial positions in *C. obtusa*. Thus, the optimal selection age should be considered for the improvement of wood properties through family selection. Based on the results of age–age correlation (Table 7) and heritability (Table 8), the selection of ages from the 13th to 21st radial position is considered reasonable because of the high age–age correlation and broad-sense heritability of many wood properties in *C. obtusa*. In MFA, air-dry density, MOE, MOR, and compressive strength, the highest heritability was obtained in mature wood (22nd–34th radial position). This tendency for heritability to be higher in mature wood than in juvenile wood is in accordance with that of previous studies [5–7]. In *C. obtusa*, the improvement of wood quality in mature wood is considered to be more effective than that in juvenile wood by tree breeding for wood quality.

**Table 9** Loading values of principal component analysis for six families

| Variable | Juvenile wood | | Mature wood | |
|---|---|---|---|---|
| | PC1 | PC2 | PC1 | PC2 |
| Load at proportional limit | 0.666 | – 0.152 | – 0.371 | 0.655 |
| Deflection at proportional limit | 0.287 | 0.671 | 0.498 | 0.534 |
| Maximum load | 0.671 | 0.026 | – 0.539 | 0.407 |
| Maximum deflection | – 0.150 | 0.725 | 0.569 | 0.346 |

PC1 and PC2 are the first and second principal components, respectively

### Classification of load–deflection curves

The loading values of principal components are listed in Table 9, and a plot of principal component scores and a cluster dendrogram are shown in Fig. 3. In juvenile wood, load and deflection mainly contributed to the first and second principal components, respectively (Table 9). On the other hand, the first and second principal components in mature wood were mainly related to the variables of proportional limit and maximum load, respectively (Table 9). From the cluster analysis results, six families were classified into four groups for both juvenile and mature wood (Fig. 3). Typical load–deflection curves determined by averaging four variables in each group are also illustrated in Fig. 3. As well as juvenile wood of *C. japonica* [10], the load–deflection curves of juvenile wood of *C. obtusa* were classified according to differences in the proportional limit and amount of deflection in the plastic region. The load–deflection curve LDC-I in juvenile wood in Fig. 3 had a lower load at the proportional limit and larger deflection in the plastic region. Compared to LDC-I in juvenile wood, the other three types of load–deflection curve showed a higher load at the proportional limit with different amounts of deflection in the plastic region. In mature wood, LDC-I exhibited a similar load–deflection curve to LDC-I in juvenile wood (Fig. 3). LDC-III showed a higher load at the proportional limit and a smaller deflection in the plastic region. Both LDC-II and LDC-IV exhibited intermediate loads at the proportional limit between LDC-I and LDC-III, but deflection in the plastic region differed between LDC-II (smaller deflection) and LDC-IV (larger deflection). Based on the results, it is considered that load–deflection

(See figure on next page.)

**Fig. 3** A plot of principal component scores, cluster dendrogram, and shape of typical load–deflection curves for juvenile and mature wood. Note: PC1 and PC2 are the first and second principal components, respectively. The plotted codes in the top figure are Family ID. The vertical axis in the middle figure shows the distance between families based on the squared Euclidean distance using the Ward hierarchical clustering algorithm. Family groups I, II, III, and IV show types of load–deflection curve described as LDC-I, LDC-II, LDC-III, and LDC-IV in the bottom figure, respectively. Load–deflection curves of LDC-I, LDC-II, LDC-III, and LDC-IV in juvenile wood were obtained from H2, S2, M5, and S in Family ID, and similarly in mature wood, from H2, S2, S, and T2 in Family ID, respectively.

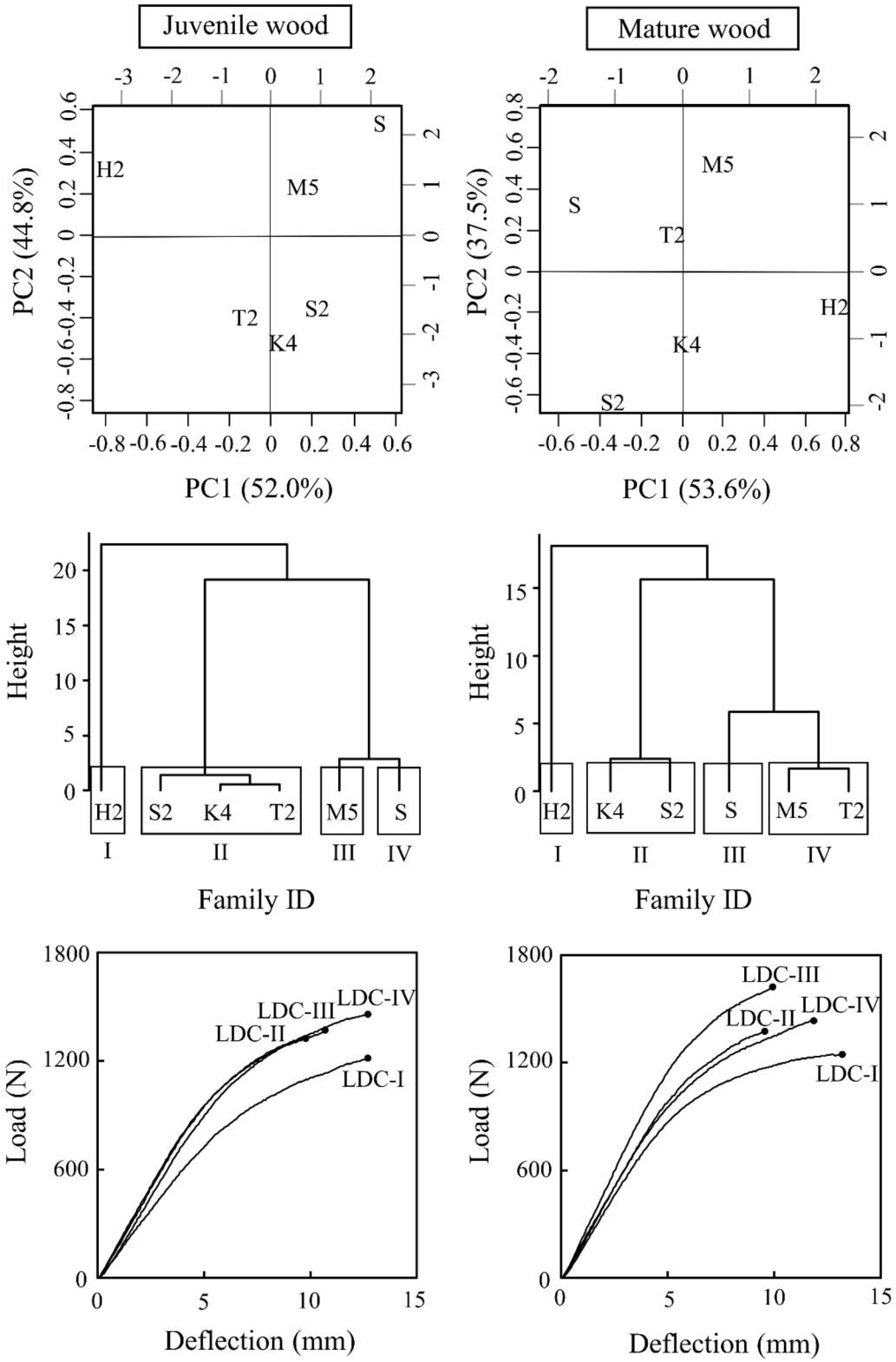


**Fig. 3** (See legend on previous page.)

curves in *C. obtusa* families vary in mature wood compared with juvenile wood. These results were supported by the larger heritability of bending properties in mature wood (Table 8), suggesting that characteristics of plastic regions as well as elastic properties can be improved by selection of families, particularly for mature wood. Comparing the differences in load–deflection curves between juvenile and mature wood in each family, it is also considered that the properties of wood under load might change due to xylem maturation, such as from juvenile to mature wood, among families of *C. obtusa*.

## Conclusion

In the present study, radial variations of wood properties for 34-year-old trees from six half-sib families in *C. obtusa* were fitted to linear and nonlinear mixed-effects models with random effects of families. The broad-sense heritability was estimated for wood properties and mechanical properties. Correlation coefficients between wood properties and mechanical properties were also examined. The optimal model for MOE was a nonlinear mixed-effects model with random effects in slope. All mechanical properties in mature wood were highly correlated with MFA or air-dry density compared with those in juvenile wood. In addition, correlation coefficients between MFA and MOE, and between air-dry density and compressive strength were significant across the stem. These results indicate that the mechanical properties of *C. obtusa* can be estimated using both MFA and air-dry density as criteria. Moderate-to-high broad-sense heritability ($H^2 = 0.18–0.50$) was found in all wood properties, with a few exceptions. The boundary between juvenile and mature wood showed high heritability ($H^2 = 0.51$), indicating that mature wood volume can be improved by tree breeding. For almost all wood properties, higher heritability was obtained in mature wood, indicating that using wood properties in mature wood as target traits is a more desirable strategy for tree breeding for wood quality in this species. In addition, not only elastic properties but also plastic properties varied among families, especially in mature wood, suggesting that plastic properties in *C. obtusa* might be improved, as well as elastic properties such as MOE. The types of load–deflection curve in several families were different between juvenile and mature wood. Further research is needed to clarify the differences in load–deflection curves between juvenile wood and mature wood using a much larger number of families and individual trees.

**Abbreviations**

MFA: Microfibril angle; MOE: Modulus of elasticity; MOR: Modulus of rupture; AIC: Akaike information criterion; $H^2$: Broad-sense heritability.

**Acknowledgements**

The authors would like to thank Mr. Kohei Noguchi, Dr. Murzabyek Sarkhad, and Dr. Erdene-Ochir Togtokhbayar for their assistance with the field sampling and the laboratory experiments.

**Author contributions**

YT, FI, and RE designed the research layout, and IN and MM supported the statistical analysis. YT and FI collected and analyzed the data and drafted the manuscript. All authors discussed the results and conclusions and contributed to writing the final manuscript. All the authors have read and approved the final manuscript.

**Funding**

None declared.

**Availability of data and materials**

The datasets used and/or analyzed during the current study are available from the corresponding author on reasonable request.

## Declarations

**Competing interests**

The authors declare that they have no competing interests.

**Author details**

[1]School of Agriculture, Utsunomiya University, Utsunomiya 321-8505, Japan. [2]United Graduate School of Agricultural Science, Tokyo University of Agriculture and Technology, Fuchu, Tokyo 183-8509, Japan. [3]Forest Tree Breeding Center, Forestry and Forest Products Research Institute, Hitachi 319-1301, Japan. [4]Faculty of Education, Chiba University, Chiba 263-8522, Japan. [5]Forestry Research Institute, Chiba Prefectural Agriculture and Forestry Research Center, Sanbu 289-1223, Japan.

Received: 15 January 2022 Accepted: 4 April 2022
Published online: 28 April 2022

**References**

1. Forestry Agency (2021) Annual report on forest and forestry in Japan (FY2020). https://www.rinya.maff.go.jp/j/kikaku/hakusyo/R2hakusyo/attach/pdf/zenbun-64.pdf. Accessed 20 Dec 2021. in Japanese
2. Kijidani Y, Fujii Y, Kimura K, Fujisawa Y, Hiraoka Y, Kitahara R (2012) Microfibril angle and density of hinoki (*Chamaecyparis obtusa*) trees in 15 half-sib families in a progeny test stand in Kyusyu, Japan. J Wood Sci 58:195–202. https://doi.org/10.1007/s10086-011-1240-8
3. Fukatsu E, Matsunaga K, Kurahara K, Chigira Y, Takahashi M (2013) The efficiency of the evaluation of wood density using Pilodyn and the genetic relationship with growth traits in Hinoki cypress (*Chamaecyparis obtusa*) in Japan. Kyushu J For Res 66:13–16 (**in Japanese**)
4. Kijidani Y, Kawasaki Y, Matsuda D, Nakazono F, Hayakawa M, Mutaguchi H, Sakagami H (2014) Tree heights in the ring-formed years affect microfibril angles in the rings from juvenile to mature wood at breast height in hinoki trees (*Chamaecyparis obtusa*). J Wood Sci 60:381–388. https://doi.org/10.1007/s10086-014-1426-y
5. Lenz P, Cloutier A, MacKay J, Beaulieu J (2010) Genetic control of wood properties 86 in *Picea glauca*—an analysis of trends with cambial age. Can J For Res 40:703–715. https://doi.org/10.1139/X10-014
6. Chen ZQ, Gil MRG, Karlsson B, Lundqvist SO, Olsson L, Wu HX (2014) Inheritance of growth and solid wood quality traits in a large Norway spruce population tested at two locations in southern Sweden. Tree Gene Genom 10:1291–1303. https://doi.org/10.1007/s11295-014-0761-x
7. Fujimoto T, Akutsu A, Nei M, Kita K, Kuromaru M, Oda K (2006) Genetic variations in wood stiffness and strength properties of hybrid larch (*Larix gmelinii* var. *japonica* × *L. kaempferi*). J For Res 11:343–349. https://doi.org/10.1007/s10310-006-0221-z

8. Fukatsu E, Tsubomura M, Fujisawa Y, Nakada R (2013) Genetic improvement of wood density and radial growth in *Larix kaempferi*: results from a diallel mating test. Ann For Sci 70:451–459. https://doi.org/10.1007/s13595-013-0278-8
9. Sasaki H, Sumiya K, Takino PS (1983) Mechanical properties of thirty-six varieties of *Cryptomeria*. Wood Res Tech Notes 17:192–205 (**in Japanese**)
10. Takahashi Y, Futosshi I, Aiso H, Takashima Y, Hiraoka Y, Iki T, Ohshima J, Iizuka K, Yokota S (2021) Inheritance of static bending properties and classification of load-deflection curves in *Cryptomeria japonica*. Holzforschung 75:105–113. https://doi.org/10.1515/hf-2019-0316
11. Ishiguri F, Matsui R, Iizuka K, Yokota S (2008) Yoshizawa N (2008) Prediction of mechanical properties of lumber by stress-wave velocity and Pilodyn penetration of 36-year-old Japanese larch trees. Holz Roh Werkst 66:275–280. https://doi.org/10.1007/s00107-008-0251-7
12. Kobayashi Y (1952) A simple method of demonstrating the fibrillar orientation in lignified walls. J Jpn For Soc 34:392–393. https://doi.org/10.11519/jjfs1934.34.12_392. (**In Japanese**)
13. Senft JF, Bendtsen BA (1985) Measuring microfibrillar angles using light microscopy. Wood Fiber Sci 17:564–567
14. R Development Core Team (2020) R: A language and environment for statistical computing. R Foundation for Statistical Computing, Vienna, Austria. https://www.R-project.org/. Accessed 28 Oct 2020
15. Bates D, Mächler M, Bolker BM, Walker SC (2015) Fitting linear mixed-effects models using lme4. J Stat Softw 67:1–48. https://doi.org/10.48550/arXiv.1406.5823
16. Pinheiro JC, Bates DM (2000) Mixed-effects models in S and A-PLUS. Springer, New York
17. Tonitto C, Powell TM (2006) Development of a spatial terrestrial nitrogen model for application to Douglas-fir forest ecosystem. Ecol Modell 193:340–362. https://doi.org/10.1016/j.ecolmodel.2005.08.041
18. Auty D, Achim A (2008) The relationship between standing tree acoustic assessment and timber quality in Scots pine and the practical implications for assessing timber quality from naturally regenerated stands. Forestry 81:475–487. https://doi.org/10.1093/forestry/cpn015
19. Akaike H (1998) Selected papers of Hirotugu Akaike. In: Parzen E, Tanabe K, Kitagawa G (eds) Springer series in statistics. Springer, New York
20. Jain AK, Dubes RC (1988) Algorithms for clustering data. Prentice-Hall, Englewood Cliffs
21. Sumiya K, Shimaji K, Itoh T, Kuroda H (1982) A consideration on some physical properties of Japanese cedar (*Cryptomeria japonica* D. Don) and Japanese cypress (*Chamaecyparis obtusa* S. and Z.) planted at different densities. Mokuzai Gakkaishi 28:255–259 (**in Japanese and English summary**)
22. Koga S, Oda J, Tsutsumi J, Koga H (1992) Wood properties variations with a stand of hinoki (*Chamecyparis obtusa*) and karamatsu (*Larix kaempferi*). Bull Kyusyu Univ For 66:55–68 (**in Japanese and English summary**)
23. Ishiguri F, Kawashima M, Iizuka K, Yokota S, Yoshizawa N (2006) Relationship between stress-wave velocity of standing tree and wood quality in 27-year-old hinoki (*Chamaecyparis obtusa* Endl). J Soc Mater Sci, Jpn 55:576–582. https://doi.org/10.2472/jsms.55.576 (**in Japanese and English summary**)
24. Tsushima S, Fujioka Y, Oda K, Matsumura J, Shiraishi S (2006) Variations of wood properties in forests of seedlings and cutting cultivars of hinoki (*Chamaecyparis obtusa*). Mokuzai Gakkaishi 52:277–284. https://doi.org/10.2488/jwrs.52.277 (**in Japanese and English summary**)
25. Ido H, Nagao H, Kato H (2012) Strength properties of Japanese cypress (*Chamaecyparis obtusa*) pithless lumber and small clear specimens sawn from a large diameter log. Bull For For Prod Res Inst 11:121–133 (**in Japanese and English summary**)
26. Panshin AJ, de Zeeuw C (1980) Textbook of wood technology. McGraw-Hill Book, New York
27. Bendtsen BA, Senft J (1986) Mechanical and anatomical properties in individual growth rings of plantation-grown eastern cottonwood and loblolly pine. Wood Fiber Sci 18:23–38
28. Zobel BJ, van Buijtenen JP (1989) Wood variation: its causes and control. Springer, Berlin
29. Itoh T, Yamaguchi K, Kuroda H, Shimaji K, Sumiya K (1980) The influence of planting density on the wood quality of sugi and hinoki. Wood Res Tech Notes 15:45–60 (**in Japanese**)
30. Tanabe J, Tamura A, Hamanaka M, Ishiguri F, Takashima Y, Ohshima J, Iizuka K, Yokota S (2014) Wood properties and their among-family variations in 10 open-pollinated families of *Picea jezoensis*. J Wood Sci 60:297–304. https://doi.org/10.1007/s10086-014-1407-1
31. Zhu J, Takata K, Iijima Y, Hirakawa Y (2003) Growth and wood quality of sugi (*Cryptomeria japonica*) planted in Akita Prefecture (I): Variation of some wood quality indices within tree stems. Mokuzai Gakkaishi 49:138–145 (**in Japanese and English summary**)
32. Shiokura T (1982) Extent and differentiation of the juvenile wood zone in coniferous tree trunks. Mokuzai Gakkaishi 28:85–90 (**in Japanese and English summary**)
33. Tumenjargal B, Ishiguri F, Aiso H, Yusuke T, Nezu I, Otsuka K, Ohshima J, Yokota S (2020) Physical and mechanical properties of wood and their geographic variations in *Larix sibirica* trees naturally grown in Mongolia. Sci Rep 10:12936. https://doi.org/10.1038/s41598-020-69781-7
34. Baltunis BS, Wu HX, Powell MB (2007) Inheritance of density, microfibril angle, and modulus of elasticity in juvenile wood of *Pinus radiata* at two locations in Australia. Can J For Res 37:2164–2174. https://doi.org/10.1139/X07-061
35. Cown DJ, Hebert J, Ball R (1999) Modeling *Pinus radiata* lumber characteristics: part 1: mechanical properties of small clears. N Z J For Sci 29:203–213
36. Kumar S, Jayawickrama JS, Lee J, Lausberg M (2002) Direct and indirect measures of stiffness and strength show high heritability in a wind-pollinated radiata pine progeny test in New Zealand. Silva Genet 51:256–261


## Publisher's Note